

Fabrication of porous alumina using a paraffin pore-forming agent for laser pump cavity applications

S. Afroushteh¹, F. Soleimani^{1}*

¹University of Malayer, Materials Engineering Department, Malayer, Iran

Abstract

Paraffin was employed as a pore-forming agent to achieve porous alumina. Trichloroethylene, toluene, and chloroform were utilized for dissolving paraffin to explore the impact of the solvent on the properties of porous alumina. The influence of the paraffin ratio (1, 3, 5, and 7 wt%) was also examined on the properties of porous alumina. The samples were compacted under different pressures ranging from 30 to 50 MPa. The samples were then sintered at 1400 °C. The density of the samples was examined by the Archimedes method. The porosity percentage depended on the content of the pore-forming agent and the initial pressure of the compaction process. Based on the X-ray diffraction results, the size of the crystallites was about 230 nm. The sample with 3 wt% paraffin showed the highest strength (155 MPa) which can be assigned to its proper pore size distribution. The distribution and size of the pores were investigated by a field emission scanning electron microscope. Finally, the sample prepared with 5 wt% paraffin in toluene and compacted at 40 MPa was utilized as a laser pump reflector in an Nd-YAG laser cavity. Based on the results, the reflection of the porous alumina was above 99% at the wavelength of 430 nm.

Keywords: porous alumina, pore-forming, laser cavity.

INTRODUCTION

Interest in studying porous ceramics has increased in recent decades [1-3]. The fabrication of porous ceramics will result in the development of specific applications [4, 5]. The pore size and its size distribution can be controlled in a low-density matrix to achieve a product with proper strength, low thermal conductivity, high specific surface area, and long durability. Various applications of porous ceramics include catalyst support [6], molten metal filters, the exhaust of diesel engines, flames, biomedical devices support [7, 8], and high-temperature thermal insulation [9]. Porous alumina has been employed in various applications including thermal insulators, and molten filters [10]. One of the advanced applications of porous alumina is its use as a laser resonator cavity [11]. A laser resonator cavity is used in solid-state lasers to increase efficiency, but the low efficiency of the high-power lasers has been always a serious challenge. Such a decline in the efficiency can be attributed to the lateral radiation of the laser to the surroundings. Ceramic devices, known as a cavity, are used to focus the laser beam which reflects the laser radiation in a specific wavelength [12]. The resonator cavity prevents the saturation of the scattered waves and enhances the pumping of the laser.


Various methods have been developed for the preparation of porous materials to meet the engineering requirements. These methods include sacrificing templates, extrusion, freeze-casting, direct foaming, lithography, and fast sample preparation, each with its specific advantages and

drawbacks [13]. One of the methods with wide applications in the production of porous ceramics with controlled microstructure (porosity and pore size) involves the use of pore-forming agents [14]. These agents are burnt out until the final sintering temperature of the ceramics and leave hollow pores within the ceramics. These pore-forming agents are low-cost, non-toxic, and environmentally friendly and can be properly burnt at 300-600 °C leaving behind pores with a size range of 5-50 m [15-17]. It has been shown that pore-forming species can result in pores of various types and morphologies regardless of their particle size. However, in the present research, paraffin was used as a pore-forming agent. The effect of paraffin solvent and press pressure on porous alumina has been investigated with different analysis techniques.

EXPERIMENTAL METHODS

The porous alumina was prepared by submicron alumina powder (PG 701, Indal) with a mean particle size of 0.6 m and purity of 99.6%. The particle size distribution of the alumina powder is presented in Fig. 1. The applied paraffin in this research was high-purity liquid paraffin. Paraffin cannot be directly used as the pore-forming agent in the preparation of ceramics as it can accumulate in some parts of the material due to its high viscosity, leading to improper porosity. Therefore, it must be first mixed with a proper solvent and then impregnated with the ceramic powder. Three different solvents (toluene, trichloroethylene and chloroform, reagent grades, Notron Chemicals) were used for this purpose. In a typical procedure, various weight percentages of paraffine (1-7 wt%) were dissolved in 100 mL of the mentioned solvents. Then alumina powder was added and the mixture

*f.soleimany@yahoo.com

 <https://orcid.org/0000-0003-0008-3400>

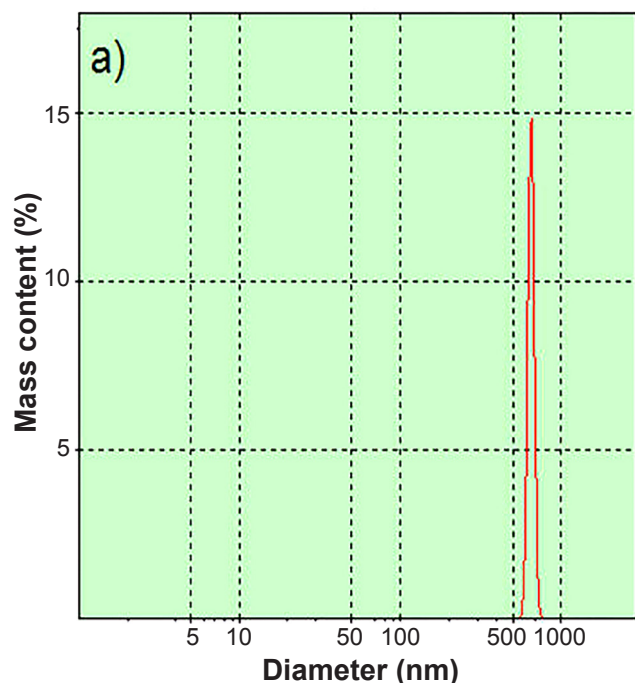


Figure 1: Particle size distribution curve of alumina powder used as a raw material.

Table I - Alumina samples with different solvents and different paraffin percentages.

Code	Solvent	Paraffin (wt%)	Alumina content (wt%)
AT1	Toluene	1	99
AT3		3	97
AT5		5	95
AT7		7	93
BT1	Trichloroethylene	1	99
BT3		3	97
BT5		5	95
BT7		7	93
CC1	Chloroform	1	99
CC3		3	97
CC5		5	95
CC7		7	93

was homogenized by a fast-mill (300 rpm) using alumina balls for 3 h. Table I presents the samples based on their solvent type. After drying the samples in an electrical dryer (at 60 °C for 24 h), the obtained powders were ground in a porcelain mortar and sieved using a mesh grade of 40. Then, 10% humidity was added and the samples were kept in a closed container to control their humidity for granulation. Then proper granules were obtained for the compaction process. In this step, the samples were compacted at various pressures of 30, 40, and 50 MPa using a cylindrical mold

with the dimensions of 35x35x20 mm. Finally, an electrical furnace with a temperature of 1400 °C (heating rate of 2 °C/min) was used for 1 h to sinter the samples at maximum sintering temperature.

The Archimedes method was employed to determine the bulk density and porosity of the samples [18]. The dry weight of the samples (D) was first measured, then, they were boiled in water for 4 h and cooled down to room temperature for 24 h, then, their wet weight (W) was measured. The floating weight of the samples (S) was then determined. The porosity and density of the samples could be calculated by the floating equations:

$$\text{Porosity} = \frac{W - D}{W - S} \quad (\text{A})$$

$$\text{Bulk density} = \frac{D (\text{water density})}{W - S} \quad (\text{B})$$

$$\text{Relative density} = \frac{\text{bulk density}}{\text{theoretical density}} \cdot 100 \quad (\text{C})$$

In this study, the theoretical density of Al_2O_3 was considered 3.98 g/cm³. X-ray diffraction (XRD) technique (PW3710, Philips, Netherlands) was employed to determine the final phases of the sample. The strength of the samples was also evaluated using the three-point bending method [19]. In order to determine the standard deviation, the experiments were repeated three times. The field emission scanning electron microscopy (FESEM) technique (MIRA3, Tescan) was also applied to assess the microstructure of the samples. Samples were cut to achieve the dimension of 10x10 mm with a thickness of 3 mm. Finally, samples were coated with a thin layer of Au before the FESEM analysis. Diffuse reflectance UV-vis spectrometry (DRS) in the visible and UV range is an efficient method to determine the reflection spectrum of solid materials [20]. The reflection of the samples was measured in the wavelength range of 200-900 nm using a spectrometer (DRS, Shimadzu).

RESULTS AND DISCUSSION

As shown in Fig. 2, the images of falcons a (toluene), b (trichloroethylene), and c (chloroform) show that solvents completely dissolved 7% paraffin, resulting in a uniform, transparent, and single-phase solution. For comparison, it was tried to solve 7% paraffin in ethanol (Fig. 2d). It is obvious that it did not dissolve. All three solvents were utilized to assess the effect of the solvent on the physical and mechanical properties of the porous samples. Paraffin has been already used as a pore-forming agent in porous ceramics [21]; however, its optimal percentage in each ceramic sample depends on the specifications of the corresponding ceramic powder. Low contents of pore-forming agent results in low-porosity samples; while over-consumption of this agent leads to a porous material with large pores and poor strength.

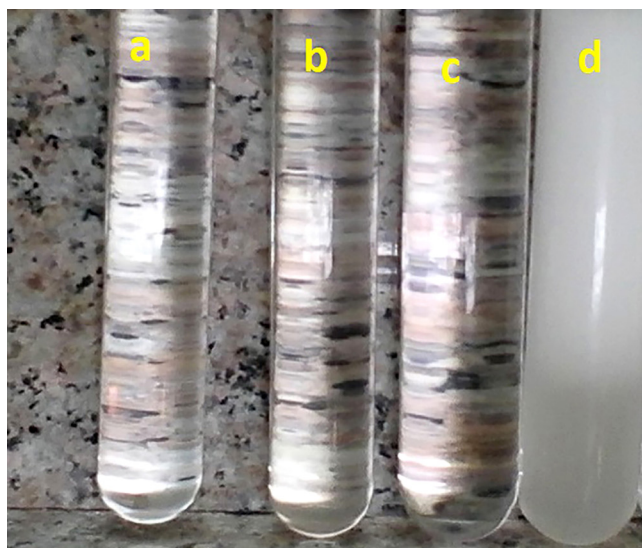


Figure 2: Photo showing the results of dissolving paraffin in: a) toluene; b) trichloroethylene; c) chloroform; and d) ethanol.

Therefore, the determination of the precise amount of the pore-forming agent is of crucial significance.

As mentioned, the compaction pressure plays a decisive role in the level of porosity in the porous sample. Although higher pressure has been shown to increase the density and decrease the porosity [22], very low pressures cannot be

Table II - Density and porosity of AT3 sample with different compaction pressure.

Pressure (MPa)	Density (g/cm ³)	Porosity (%)
30	3.25±0.05	9.14±0.10
40	3.34±0.03	7.21±0.05
50	3.41±0.05	5.20±0.05

considered to achieve high porosity as the final device will not have proper strength. The samples were first prepared at three different pressures of 30, 40, and 50 MPa. Their total porosity and bulk density were then measured as listed in Table II for sample AT3. Based on the data obtained from Archimedes equation, lower pressure led to lower density and higher porosity percentage and vice versa. According to the results, low pressure resulted in lower density and non-uniform porosity, while very high pressure led to the accumulation of paraffin, giving rise to irregular porosity. Although the pressure level of 30 MPa resulted in higher porosity in the sample, the samples experienced cracking and chipping during the transition due to their low green strength. Therefore, the pressure of 40 MPa was selected for continuing the research and the subsequent samples were compacted at the pressure of 40 MPa.

As listed in Table III, generally, the porosity increased by enhancing the percentage of paraffin in all three solvents. As we know, the water absorption depends on the amount of the open pores in the samples. On the other hand, significant changes can be observed in the mechanical strength of the samples. It must be noted that there are some reports on the strength obtained by pore-forming agents such as carbon black or wheat flour which showed lower strengths compared to the present research at the same level of porosity [14]. The highest flexural strength was detected in the sample AT3. In the case of optical cavities, the strength must be high as the device is exposed to thermomechanical shocks due to temperature variations [12]. Therefore, it seems that the sample with 3 wt% paraffin is suitable for laser cavity applications. In the case of the use of the device in thermal insulation, the sample containing 7 wt% paraffin is ideal as its porosity is about 16%. Comparing the samples with 3 wt% paraffin prepared by three different solvents, the sample fabricated by toluene exhibited higher strength which can be assigned to the shape and distribution of the pores in these samples. This shows the necessity of microstructural studies.

Table III - Densitometry results and bending strength of the samples.

Code	Density (g/cm ³)	Porosity (%)	Water absorption (%)	Bending strength (MPa)
AT1	3.27±0.03	13.23±0.07	4.00±0.05	103±8
AT3	3.34±0.03	7.21±0.04	1.80±0.03	155±12
AT5	3.36±0.04	14.31±0.05	3.30±0.05	47±4
AT7	3.10±0.05	16.35±0.13	5.20±0.07	12±3
BT1	3.29±0.03	13.67±0.09	4.10±0.05	159±15
BT3	3.36±0.05	7.32±0.05	4.00±0.05	87±9
BT5	3.14±0.03	15.52±0.18	5.20±0.09	32±6
BT7	3.02±0.02	16.26±0.16	3.70±0.08	5±1
CC1	3.21±0.04	14.61±0.13	4.60±0.05	125±8
CC3	3.51±0.05	7.58±0.05	2.10±0.03	90±9
CC5	3.15±0.03	15.07±0.15	4.70±0.07	28±5
CC7	3.07±0.02	15.92±0.23	5.10±0.05	12±3

The samples were evaluated by XRD to assess their phases. Fig. 3 shows the XRD patterns of AT3, BT3, and

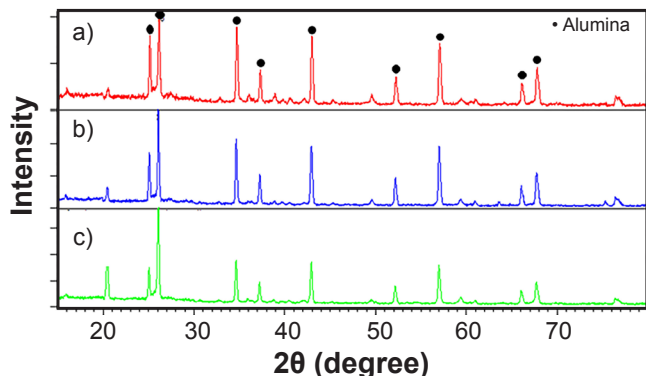


Figure 3: XRD patterns of the samples: a) AT3; b) BT3; and c) CC3.

CC3 samples all of which similarly show corundum phase. The crystallite size of the samples was determined by the Debye-Scherrer equation [23] which ranged from 220 to 230 nm. The optimum crystallite size of alumina as a laser reflector, is a function of the wavelength of the radiation being pumped. For a pump band of 0.4-2 μm , crystallite size between about 0.2-0.5 μm is optimum [24, 25]. Thus, the crystallite sizes of the samples were good enough for laser reflecting. Regarding these similarities, the microstructure of the samples should be evaluated. Fig. 4 depicts the FESEM images of the fracture cross-section of the porous alumina samples with various contents of paraffin (AT1, AT3, AT5, and AT7). The presence of micron-sized pores can be observed in all four images which were formed as a result of the paraffin burning out. The porosity due to the pore-forming agent can be seen in these figures. The higher the

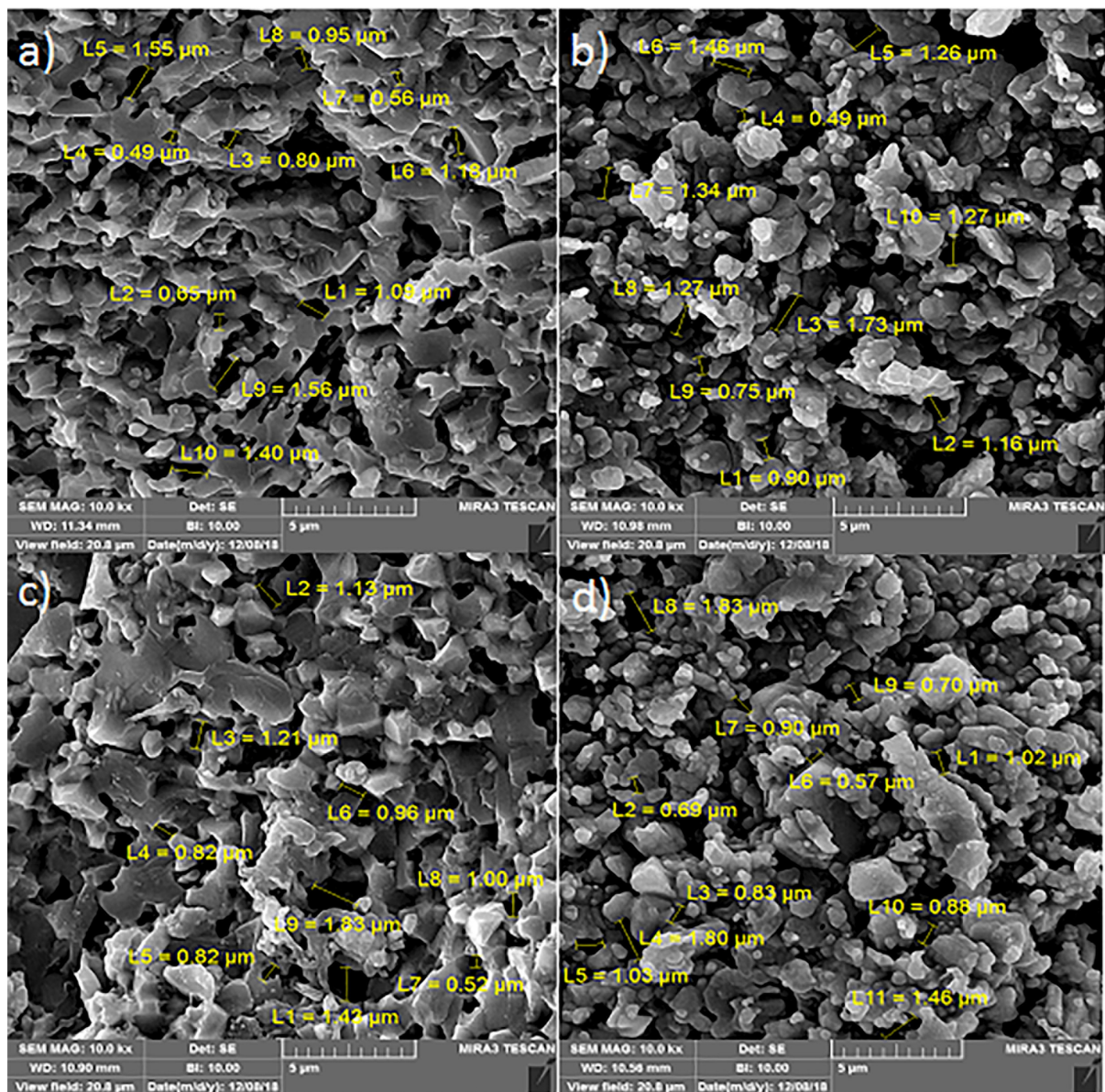


Figure 4: FESEM images of the fracture cross-section of the porous alumina samples with various contents of paraffin dissolved in toluene: a) AT1; b) AT3; c) AT5; and d) AT7.

content of the pore-forming agent, the larger the pore size. The microstructure of these samples indicated submicron pore size. A rise in the paraffin percentage in the toluene solvent increased the mean pore size from 0.8 to 1.3 μm . The density of the samples prepared with 1% and 7% of pore-forming agent was similar which can be attributed to the uniform distribution of paraffin in the samples containing lower amounts of paraffin compared to those having higher levels of this agent. By enhancing the paraffin additive from 1 wt% in the AT1 sample to 7 wt% in the AT7 sample, the pore size increased. Such increment can be attributed to the rise in the linkage between paraffin particles by elevating its content which enlarged the pore size. The open channels and pathways between the pores increased by enhancing paraffin content, showing a proper agreement with the distribution of

the pore size in these samples.

Fig. 5 illustrates the microstructure of the porous samples made by paraffin dissolved in trichloroethylene. The larger and more continuous pores, relative to sample BT7, can be observed in Fig. 5d. The presence of these larger pores as well as the open pores led to lower strength [26] which was confirmed previously in the flexural strength measurement of the samples. As mentioned before, although the presence of interconnected pores is essential in catalytic applications, for some applications the high strength is also of crucial significance. Hasselman [27] proposed the following relationship between the strength and porosity percentage:

$$\sigma = \sigma_0 - c.P \quad (D)$$

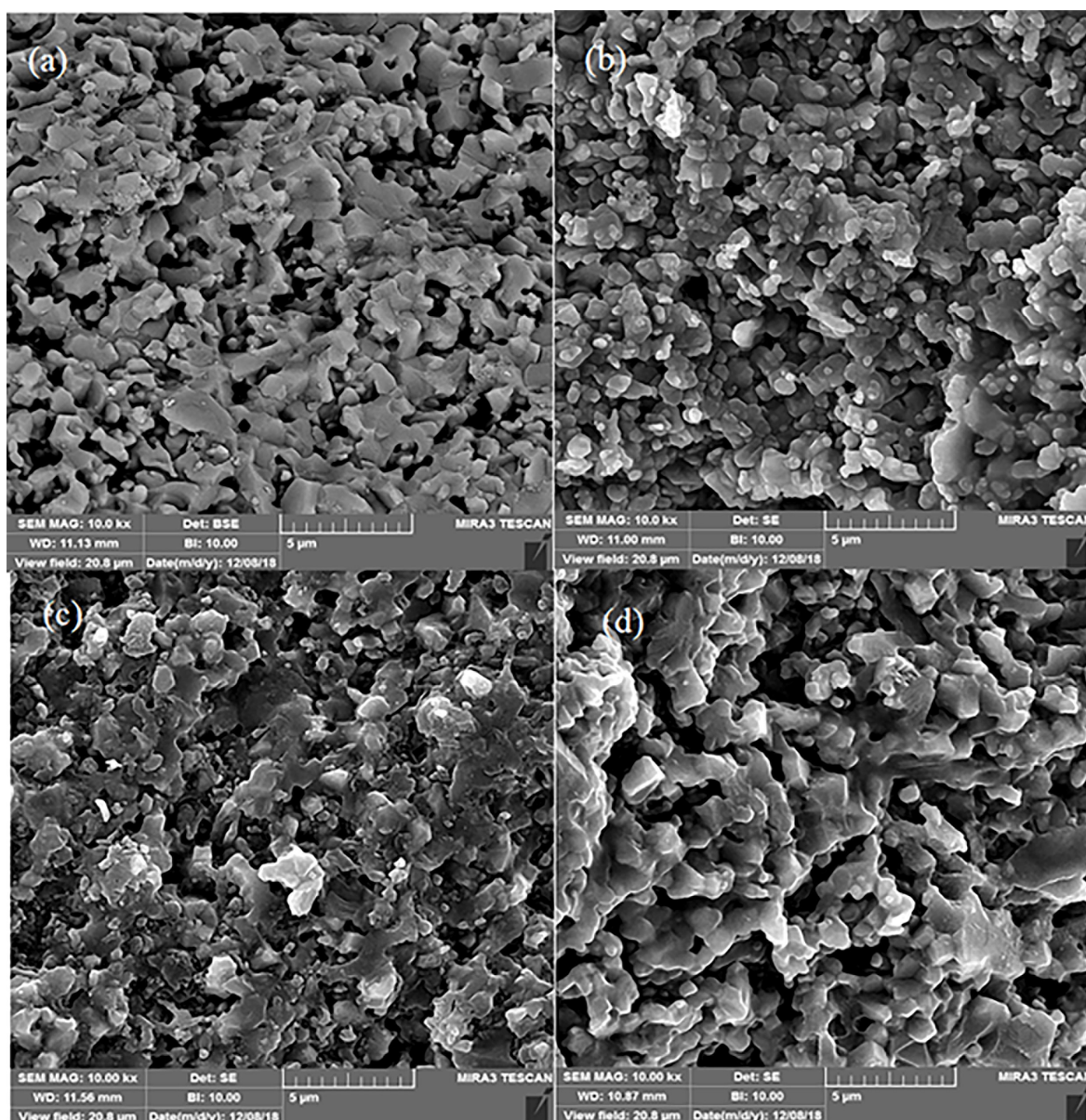


Figure 5: FESEM images showing the microstructure of the porous samples made by paraffin dissolved in trichloroethylene: a) BT1; b) BT3; c) BT5; and d) BT7.

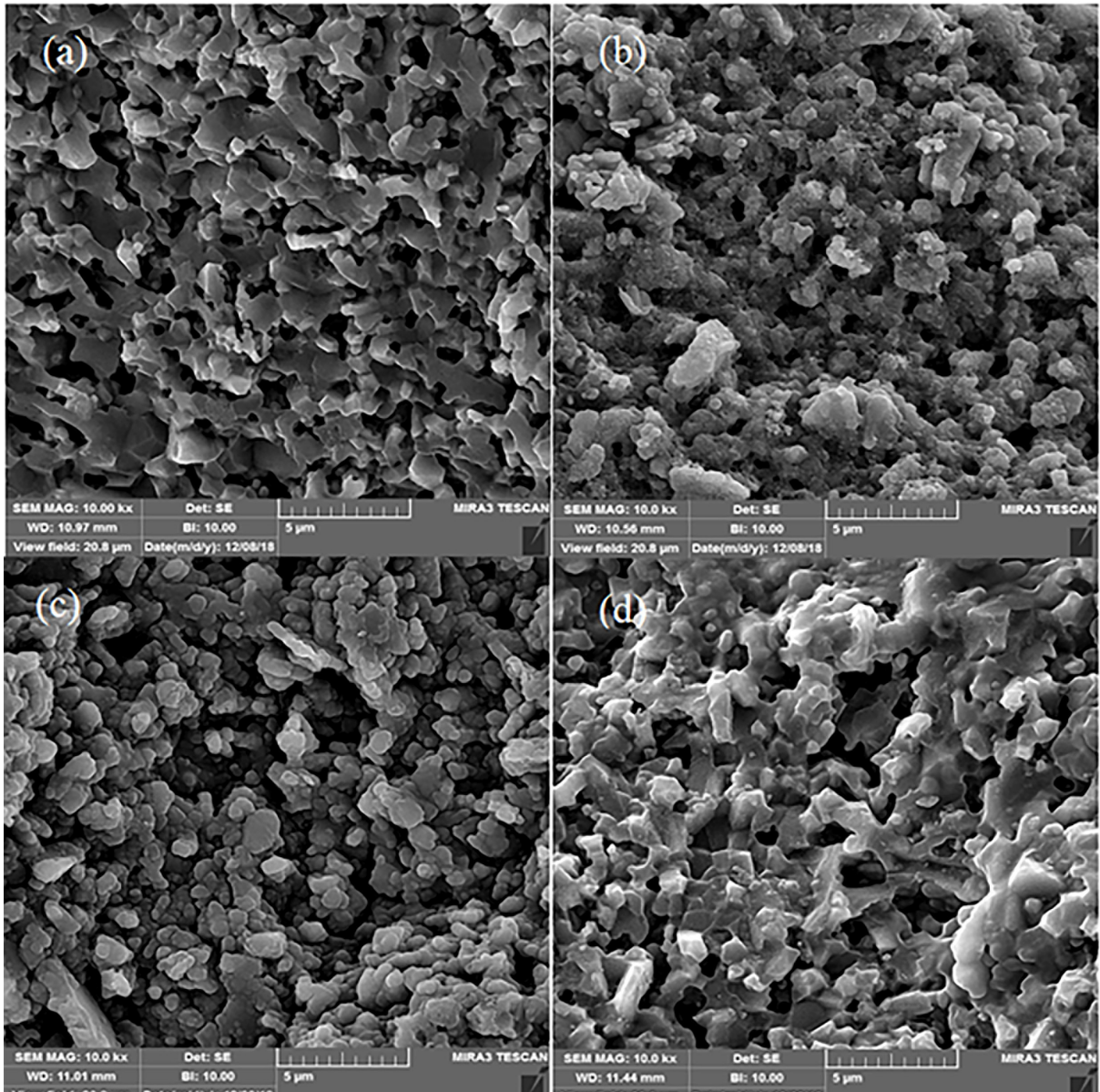


Figure 6: FESEM images showing the microstructure of the porous samples made by paraffin dissolved in chloroform: a) CC1; b) CC3; c) CC5; and d) CC7.

in which P stands for the porosity percentage whose increase linearly decreases the strength (σ). Newer theories, however, show that the strength is exponentially related to the porosity percentage in porous ceramics [26].

Fig. 6 indicates that the chloroform solvent led to more interconnected and larger pores in the ceramic which can be assigned to the lower boiling point of chloroform (61 °C) compared to that of toluene (110 °C) and trichloroethylene (82 °C). The lower boiling point results in higher vapor pressure and faster release of the pore-forming agent, leading to coarser, more irregular, and interconnected pores. On the other hand, both trichloroethylene and chloroform are more expensive and dangerous compared to toluene, further limiting their application. Therefore, toluene was a better and more effective solvent to achieve robust porous

alumina. SEM micrographs also showed that liquid phase sintering occurred; it was shown in the previous studies that even low content of impurities, for example, silica and alkaline material, in the raw material can cause glass formation in the grain boundaries during the sintering of alumina ceramics [28]. The raw material in this study was alumina, 99.6% purity, which contained silica, Na_2O , and Fe_2O_3 impurities. These impurities can form glass in the grain boundaries.

For the investigation of laser reflectivity, the reflection spectra of the samples were recorded. Fig. 7 shows the reflection curves vs. wavelength for various alumina bodies (AT1, AT3, AT5, and AT7). As can be seen, all the curves were almost similar and reflection was above 95%, close to 100% in many ranges, in the desired range (after UV range).

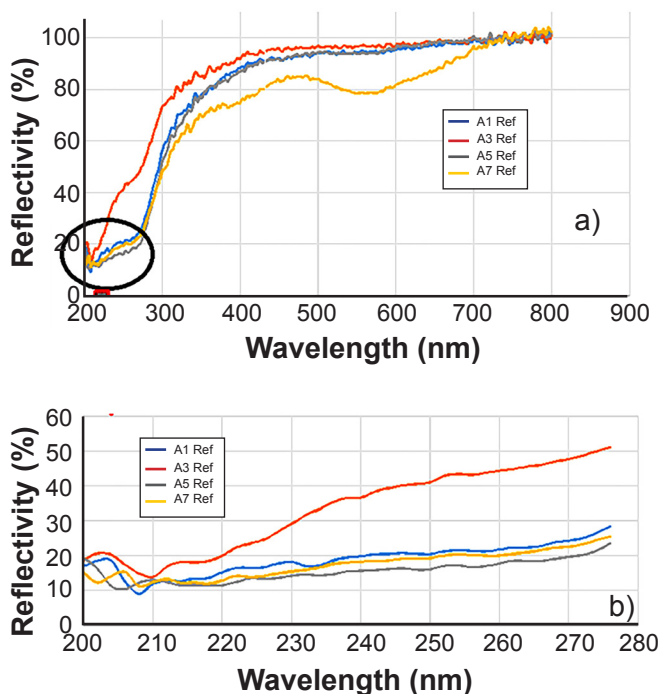


Figure 7: The reflection curves vs. wavelength for various alumina bodies: AT1, AT3, AT5, and AT7.

The alumina body and properties of alumina are the main reasons for the high reflection of these cavities in the desired range. It seems that the body with a total porosity of 15% (AT5) had proper reflection and led to desirable results. The minimum reflection in the AT1 sample was about 17% at 200 nm; at the wavelength of 600 nm, reflection rose to about 100% and the curve converted into a smooth line. At higher wavelengths, the reflection was maintained near 100%. For the AT3 sample, the minimum reflection (20%) was observed at 200 nm; the reflection rose and reached about 100% at 440 nm, beyond which the reflection remained about 100% and the reflection curve got smooth. In the case of the AT5 sample, the minimum reflection was about 16% at 200 nm; the reflection then increased and reached about 100% at 580 nm, beyond which the reflection remained almost constant (about 100%). The minimum reflection of the AT7 sample was 12% occurring at 200 nm, the reflection increased at 700 nm and reached close to 100%, beyond which the reflection remained almost 100% and the curve got into a smooth line. In the optimal sample, reflection reached its maximum at the wavelength of 440 nm and remained constant thereafter. Maximum reflection of AT1, AT3, AT5, and AT7 samples was observed at 600, 440, 580, and 700 nm, respectively.

CONCLUSIONS

Porous alumina was successfully prepared with the help of a paraffin pore-forming agent. Three types of solvents (trichloroethylene, toluene, and chloroform) were used to dissolve paraffin. Toluene was found as the most suitable solvent for dissolving paraffin since it resulted in the best

pore distribution and the highest strength. The sample prepared with paraffin content of 5 wt% and compacted at a pressure of 40 MPa showed a porosity of about 16% and a flexural strength of 47 MPa. UV-vis diffuse reflectance spectra of the samples indicated that the reflection of the optimal sample exceeded 99% at wavelengths above 430 nm, making it suitable for laser cavity applications.

REFERENCES

- [1] M. Scheffler, P. Colombo (Ed.), "Cellular ceramics: structure, manufacturing, properties and applications", Wiley (2006).
- [2] F. Soleimani, M. Rezvani, *Adv. Ceram. Prog.* **6** (2020) 36.
- [3] F. Soleimani, M. Rezvani, *Adv. Ceram. Prog.* **3** (2017) 26.
- [4] X. Li, S. Li, Z. Yin, W. Shi, M. Tao, W. Liu, Z. Gao, C. Ma, *Ceram. Int.* **49** (2023) 6873.
- [5] Z. Li, Z. Xu, Z. Ma, S. Chen, H. Zhang, B. Ren, J. Yan, *Mater. Charact.* **196** (2023) 112595.
- [6] A.V. Fedorov, Y.K. Gulyaeva, *Powder Technol.* **343** (2019) 783.
- [7] F. Soleimani, M. Rezvani, *Mater. Res. Bull.* **47** (2012) 1362.
- [8] Y. Javadzadeh, R.B. Atashgah, M. Barzegar-Jalali, F. Soleimani, G. Mohammadi, A. Sabzevari, K. Adibkia, *Colloids Surf. B Biointerfaces* **116** (2014) 751.
- [9] X. Zhang, J. He, L. Han, Z. Huang, K. Xu, W. Cai, S. Wu, Q. Jia, H. Zhang, S. Zhang, *J. Eur. Ceram. Soc.* **43** (2023) 37.
- [10] E. Gregorová, Z. Živcová, W. Pabst, *Starch* **61** (2009) 495.
- [11] M. Kojima, K. Sutoh, "Diffusion reflector", US5263042A, USA (1991).
- [12] A. Krajewski, P. Mazzinghi, *J. Mater. Sci.* **29** (1994) 232.
- [13] D.A. Hirschfeld, T.K. Li, D.M. Liu, *Key Eng. Mater.* **115** (1995) 65.
- [14] J. Liu, Y. Li, Y. Li, S. Sang, S. Li, *Ceram. Int.* **42** (2016) 8221.
- [15] E. Gregorová, W. Pabst, *J. Eur. Ceram. Soc.* **31** (2011) 2073.
- [16] S. Li, C.-A. Wang, J. Zhou, *Ceram. Int.* **39** (2013) 8833.
- [17] G. Pia, L. Casnedi, U. Sanna, *Ceram. Int.* **41** (2015) 6350.
- [18] P. Dehghani, F. Soleimani, *Ceram. Int.* **48** (2022) 16800.
- [19] D.W. Richerson, *Modern ceramic engineering: properties, processing, and use in design*, 3rd ed., Taylor Francis (2005).
- [20] M. Aceto, E. Calà, F. Gulino, F. Gullo, M. Labate, A. Agostino, M. Picollo, *Molecules* **27** (2022) 4716.
- [21] M.S. Ali, M.A.A. Hanim, S.M. Tahir, C.N.A. Jaafar, M. Norkhairunnisa, K.A. Matori, *J. Ceram. Soc. Japan* **125** (2017) 402.
- [22] M.N. Rahaman, *Ceramic processing and sintering*, 2nd ed., CRC Press (2003).

- [23] T. Alizadeh, F. Soleimani, J. Non. Cryst. Solids **520** (2019) 119465.
- [24] H. Furuse, N. Horiuchi, B.-N. Kim, Sci. Rep. **9** (2019) 10300.
- [25] Y.T. O, J.B. Koo, K.J. Hong, J.S. Park, D.C. Shin, Mater. Sci. Eng. A **374** (2004) 191.
- [26] X. Chen, S. Wu, J. Zhou, Constr. Build. Mater. **40** (2013) 869.
- [27] D.P.H. Hasselman, J. Am. Ceram. Soc. **52** (1969) 457.
- [28] I.-J. Bae, S. Baik, J. Am. Ceram. Soc. **80** (2005) 1149. (*Rec. 02/02/2023, Rev. 05/06/2023, Ac. 13/06/2023*)

